Hot topics from Belle experiment

K. Ikado
Nagoya University, Nagoya, 464-8602, Japan

We present the first evidence of the decay $B^- \to \tau^- \bar{\nu}_\tau$, using 414 fb^{-1} of data collected at the $\Upsilon(4S)$ resonance with the Belle detector at the KEKB asymmetric-energy e^+e^- collider. Events are tagged by fully reconstructing one of the B mesons in hadronic modes. We detect the signal with a significance of 4.0 standard deviations including systematics, and measure the branching fraction to be $\mathcal{B}(B^- \to \tau^- \bar{\nu}_\tau) = (1.06^{+0.34}_{-0.28}(\mathrm{stat})^{+0.22}_{-0.25}(\mathrm{syst})) \times 10^{-4}$. We also report results based on 1.86fb^{-1} data collected by the Belle detector at the $\Upsilon(5S)$ resonance. Several exclusive B_s decays $B_s \to D_s^{(*)+}\pi^-(\rho^-)$ and $B_s \to J/\psi\phi(\eta)$ are studied. The B_s meson production is found to proceed predominantly through the creation of $B_s^* \bar{B}_s^*$ pairs. Upper limits on $B_s \to K^+K^-$, $B_s \to \phi\gamma$, $B_s \to \gamma\gamma$ and $B_s \to D_s^{(*)+} D_s^{(*)-}$ decays are also reported.

1. Introduction

In the Standard Model (SM), the purely leptonic decay $B^- \to \tau^- \bar{\nu}_\tau$ proceeds via annihilation of b and $\overline{u}$ quarks to a W^- boson. It provides a direct determination of the product of the B meson decay constant f_B and the magnitude of the Cabibbo-Kobayashi-Maskawa (CKM) matrix element $|V_{ub}|$. The branching fraction is given by

$$\mathcal{B}(B^- \to \tau^- \bar{\nu}_\tau) = \frac{G_F^2 m_B m_\tau^2}{8\pi} \left(1 - \frac{m_\tau^2}{m_B^2}\right)^2 f_B^2 |V_{ub}|^2 \tau_B, \quad (1)$$

where G_F is the Fermi coupling constant, m_B and m_τ are the B and τ masses, respectively, and τ_B is the B^- lifetime [1]. Physics beyond the SM, such as supersymmetry or two-Higgs doublet models, could modify $\mathcal{B}(B^- \to \tau^- \bar{\nu}_\tau)$ through the introduction of a charged Higgs boson [2]. Purely leptonic B decays have not been observed in past experiments. The most stringent upper limit on $B^- \to \tau^- \bar{\nu}_\tau$ comes from the BaBar experiment: $\mathcal{B}(B^- \to \tau^- \bar{\nu}_\tau) < 2.6 \times 10^{-4}$ (90% C.L.) [3].

The possibility to study decays of B_s at very high luminosity e^+e^- colliders running at the energy of the $\Upsilon(5S)$ resonance has been discussed in several theoretical papers [4, 5]. The first data at the $\Upsilon(5S)$ were taken many years ago at CESR [6–8], but the collected data sample was not enough to observe a B_s signal. In 2003, the CLEO experiment collected 0.42 fb^{-1} at the $\Upsilon(5S)$ and observed some evidence for B_s meson production in both inclusive and exclusive modes. However, simple calculations assuming an approximate $SU(3)$ symmetry indicate that many interesting B_s measurements require a data sample of at least 20 pb^{-1}, which can be collected by B Factories in the future. To test the experimental feasibility of such measurements, a data sample of 1.86 fb^{-1} was recently taken with the Belle detector at the center-of-mass (CM) energy corresponding to the mass of the $\Upsilon(5S)$ resonance. This data sample is more than four times larger than the CLEO dataset at the $\Upsilon(5S)$.

The Belle detector is a large-solid-angle magnetic spectrometer consisting of a silicon vertex detector, a 50-layer central drift chamber (CDC), a system of aerogel threshold Čerenkov counters (ACC), time-of-flight scintillation counters (TOF), and an electromagnetic calorimeter comprised of CsI(Tl) crystals (ECL) located inside a superconducting solenoid coil that provides a 1.5 T magnetic field. An iron flux-return located outside of the coil is instrumented to identify K_L^0 and muons. The detector is described in detail elsewhere [9].

2. Evidence of the Purely Leptonic Decay $B^- \to \tau^- \bar{\nu}_\tau$

We use a 414 fb^{-1} data sample containing 447×10^6 B meson pairs collected with the Belle detector at the KEKB asymmetric-energy e^+e^- (3.5 on 8 GeV) collider operating at the $\Upsilon(4S)$ resonance ($\sqrt{s} = 10.58$ GeV).

We use a detailed Monte Carlo (MC) simulation, which fully describes the detector geometry and response based on GEANT [10], to determine the signal selection efficiency and to study the background. In order to reproduce effects of beam background, data taken with random triggers for each run period are overlaid on simulated events. The $B^- \to \tau^- \bar{\nu}_\tau$ signal decay is generated by the EvtGen package [11]. To model the background from $e^+e^- \to B\overline{B}$ and continuum $q\overline{q}$ ($q = u, d, s, c$) production processes, large $B\overline{B}$ and $q\overline{q}$ MC samples corresponding to about twice the data sample are used. We also use MC samples for rare B decay processes, such as charmless hadronic, radiative, electroweak decays and $b \to u$ semileptonic decays.

We fully reconstruct one of the B mesons in the event, referred to hereafter as the tag side (B_{tag}), and compare properties of the remaining particle(s), referred to as the signal side (B_{sig}), to those expected for signal and background. The method allows us to suppress strongly the combinatorial background from both $B\overline{B}$ and continuum events. In order to avoid ex-

perimental bias, the signal region in data is not looked at until the event selection criteria are finalized.

The $B_{\rm tag}$ candidates are reconstructed in the following decay modes: $B^+ \to \overline{D}^{(*)0}\pi^+$, $\overline{D}^{(*)0}\rho^+$, $\overline{D}^{(*)0}a_1^+$ and $\overline{D}^{(*)0}D_s^{(*)+}$. The $\overline{D}$ mesons are reconstructed as $\overline{D}^0 \to K^+\pi^-$, $K^+\pi^-\pi^0$, $K^+\pi^-\pi^+\pi^-$, $K^0_S\pi^0$, $K^0_S\pi^-\pi^+$, $K^0_S\pi^-\pi^+\pi^0$ and K^-K^+, and the D_s^+ mesons are reconstructed as $D_s^+ \to K^0_S K^+$ and $K^+K^-\pi^+$. The $\overline{D}^{*0}$ and D_s^{*+} mesons are reconstructed in $\overline{D}^{*0} \to \overline{D}^0\pi^0, \overline{D}^0\gamma$, and $D_s^{*+} \to D_s^+\gamma$ modes. The selection of $B_{\rm tag}$ candidates is based on the beam-constrained mass $M_{\rm bc} \equiv \sqrt{E^2_{\rm beam} - p^2_B}$ and the energy difference $\Delta E \equiv E_B - E_{\rm beam}$. Here, E_B and p_B are the reconstructed energy and momentum of the $B_{\rm tag}$ candidate in the e^+e^- center-of-mass system, and $E_{\rm beam}$ is the beam energy in the CM frame. The selection criteria for $B_{\rm tag}$ are defined as $M_{\rm bc} > 5.27$ GeV/c^2 and -80 MeV $< \Delta E < 60$ MeV. If an event has multiple $B_{\rm tag}$ candidates, we choose the one having the smallest χ^2 based on deviations from the nominal values of ΔE, the D candidate mass, and the $D^* - D$ mass difference if applicable.

In the events where a $B_{\rm tag}$ is reconstructed, we search for decays of $B_{\rm sig}$ into a τ and a neutrino. Candidate events are required to have one or three charged track(s) on the signal side with the total charge being opposite to that of $B_{\rm tag}$. The τ lepton is identified in the five decay modes, $\mu^-\bar{\nu}_\mu\nu_\tau$, $e^-\bar{\nu}_e\nu_\tau$, $\pi^-\nu_\tau$, $\pi^-\pi^0\nu_\tau$ and $\pi^-\pi^+\pi^-\nu_\tau$, which taken together correspond to 81% of all τ decays [1]. The muon, electron and charged pion candidates are selected based on information from particle identification devices. The leptons are selected with requirements that have efficiencies greater than 90% for both muons and electrons in the momentum region above 1.2 GeV/c, and misidentification rates of less than 0.2%(1.5%) for electrons (muons) in the same momentum region. Kaon candidates are rejected for all charged tracks on the signal side. The π^0 candidates are reconstructed by requiring the invariant mass of two γ's to satisfy $|M_{\gamma\gamma} - m_{\pi^0}| < 20$ MeV/c^2. For all modes except $\tau^- \to \pi^-\pi^0\nu_\tau$, we reject events with π^0 mesons on the signal side. All the selection criteria have been optimized to achieve the highest sensitivity in MC.

The most powerful variable for separating signal and background is the remaining energy in the ECL, denoted as $E_{\rm ECL}$, which is sum of the energy of photons that are not associated with either the $B_{\rm tag}$ or the π^0 candidate from the $\tau^- \to \pi^-\pi^0\nu_\tau$ decay. For signal events, $E_{\rm ECL}$ must be either zero or small value arising from beam background hits, therefore, signal events peak at low $E_{\rm ECL}$. On the other hand, background events are distributed toward higher $E_{\rm ECL}$ due to the contribution from additional neutral clusters.

The $E_{\rm ECL}$ signal region is optimized for each τ decay mode based on the MC simulation, and is defined by $E_{\rm ECL} < 0.2$ GeV for the $\mu^-\bar{\nu}_\mu\nu_\tau$, $e^-\bar{\nu}_e\nu_\tau$ and $\pi^-\nu_\tau$ modes, and $E_{\rm ECL} < 0.3$ GeV for the $\pi^-\pi^0\nu_\tau$ and $\pi^-\pi^+\pi^-\nu_\tau$ modes. The $E_{\rm ECL}$ sideband region is defined by 0.4 GeV $< E_{\rm ECL} <$ 1.2 GeV for the $\mu^-\bar{\nu}_\mu\nu_\tau$, $e^-\bar{\nu}_e\nu_\tau$ and $\pi^-\nu_\tau$ modes, and by 0.45 GeV $< E_{\rm ECL} <$ 1.2 GeV for the $\pi^-\pi^0\nu_\tau$ and $\pi^-\pi^+\pi^-\nu_\tau$ modes. Table I shows the number of events found in the sideband region for data ($N^{\rm obs}_{\rm side}$) and for the background MC simulation ($N^{\rm MC}_{\rm side}$) scaled to the equivalent integrated luminosity in data. Their good agreement for each τ decay mode indicates the validity of the background MC simulation. Table I also shows the number of the background MC events in the signal region ($N^{\rm MC}_{\rm sig}$).

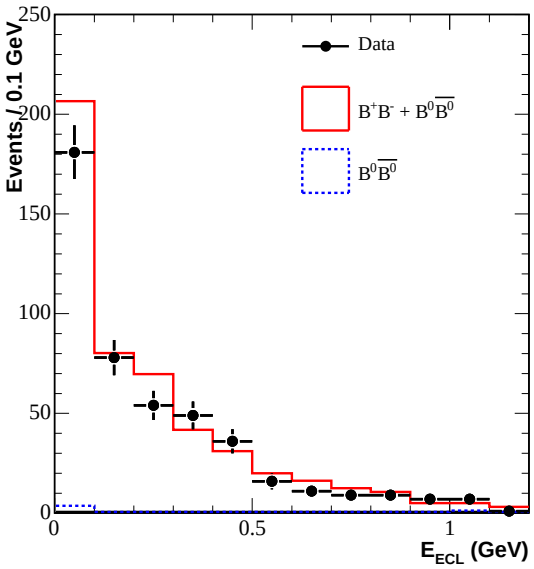

Figure 1: $E_{\rm ECL}$ distribution for the control sample of doubly tagged events, where one B is fully reconstructed and the other B is reconstructed as $B^- \to D^{*0}\ell^-\bar{\nu}$. The dots with errors indicate the data. The solid histogram represents the distribution as deduced background from $B\overline{B}$ MC ($B^+B^- + B^0\overline{B}^0$), and the dashed histogram shows the contribution from $B^0\overline{B}^0$ events.

In order to validate the $E_{\rm ECL}$ simulation, we use a control sample of events (double tagged events), where the $B_{\rm tag}$ is fully reconstructed as described above and $B_{\rm sig}$ is reconstructed in the decay chain, $B^- \to D^{*0}\ell^-\bar{\nu}$ ($D^{*0} \to D^0\pi^0$), followed by $D^0 \to K^-\pi^+$ or $K^-\pi^-\pi^+\pi^+$ where ℓ is a muon or electron. The sources affecting the $E_{\rm ECL}$ distribution in the control sample are similar to those affecting the $E_{\rm ECL}$ distribution in the signal MC simulation. Figure 1 shows the $E_{\rm ECL}$ distribution in the control sample for data and the MC simulation scaled to equivalent integrated luminosity in data. Their agreement demonstrates the validity of the $E_{\rm ECL}$ simulation in the signal MC.

After finalizing the signal selection criteria, the sig-

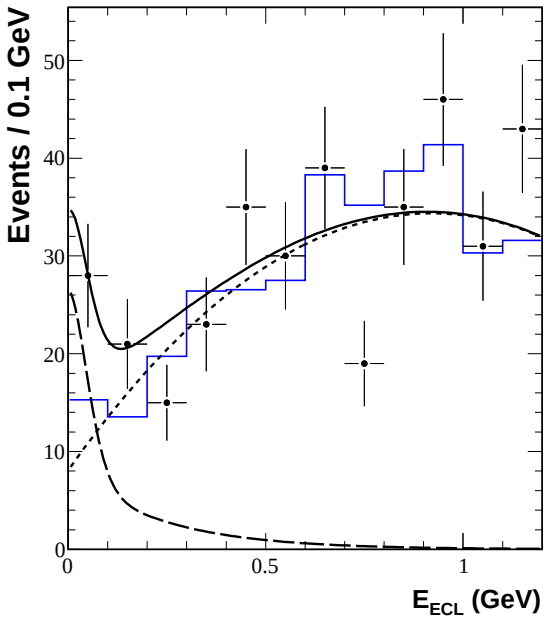

Figure 2: $E_{\rm ECL}$ distributions in the data after all selection requirements except the one on $E_{\rm ECL}$ have been applied. The data and background MC samples are represented by the points with error bars and the solid histogram, respectively. The solid curve shows the result of the fit with the sum of the signal shape (dashed) and background shape (dotted).

nal region is examined. Figure 2 shows the obtained $E_{\rm ECL}$ distribution when all τ decay modes are combined. One can see a significant excess of events in the $E_{\rm ECL}$ signal region below $E_{\rm ECL} < 0.25$ GeV. Table I shows the number of events observed in the signal region ($N_{\rm obs}$) for each τ decay mode. For the events in the signal region, we verify that the distributions of the event selection variables other than $E_{\rm ECL}$, such as $M_{\rm bc}$ and $p_{\rm miss}$, are consistent with the sum of the signal and background distributions expected from MC.

We deduce the final results by fitting the obtained $E_{\rm ECL}$ distributions to the sum of the expected signal and background shapes. Probability density functions (PDFs) for the signal $f_s(E_{\rm ECL})$ and for the background $f_b(E_{\rm ECL})$ are constructed for each τ decay mode from the MC simulation. The signal PDF is modeled as the sum of a Gaussian function, centered at $E_{\rm ECL} = 0$, and an exponential function. The background PDF, as determined from the MC simulation, is parametrized by a second-order polynomial. The PDFs are combined into an extended likelihood function,

$$\mathcal{L} = \frac{e^{-(n_s+n_b)}}{N!}\prod_{i=1}^{N}(n_s f_s(E_i) + n_b f_b(E_i)), \qquad (2)$$

where E_i is the $E_{\rm ECL}$ in the ith event, N is the total number of events in the data, and n_s and n_b are the signal yield and background yield to be determined by the fit. To combine likelihood functions of the five decay modes, we multiply the likelihood functions to produce the combined likelihood ($\mathcal{L}_{\rm com} = \prod_{j=1}^{5}\mathcal{L}_j$). The results are listed in Table I. The number of signal events in the signal region deduced from the fit ($N_{\rm s}$) is $21.2^{+6.7}_{-5.7}$ when all τ decay modes are combined. Table I also gives the number of background events in the signal region deduced from the fit ($N_{\rm b}$), which is consistent with the expectation from the background MC simulation ($N_{\rm sig}^{\rm MC}$).

The branching fractions are calculated as $\mathcal{B} = N_s/(2\cdot\varepsilon\cdot N_{B^+B^-})$ where $N_{B^+B^-}$ is the number of $\Upsilon(4S) \to B^+B^-$ events, assumed to be half of the number of produced B meson pairs. The efficiency is defined as $\varepsilon = \varepsilon^{\rm tag}\times\varepsilon^{\rm sel}$, where $\varepsilon^{\rm tag}$ is the tag reconstruction efficiency for events with $B^- \to \tau^-\bar{\nu}_\tau$ decays on the signal side, determined by MC to be 0.136 ± 0.001(stat)%, and $\varepsilon^{\rm sel}$ is the event selection efficiency listed in Table I, as determined by the ratio of the number of events surviving all of the selection criteria including the τ decay branching fractions over the number of fully reconstructed $B^\pm$. When all τ decay modes are combined we obtain a branching fraction of $(1.06^{+0.34}_{-0.28})\times 10^{-4}$. The branching fraction for each τ decay mode is consistent within error as shown in Table I.

Systematic errors for the measured branching fraction are associated with the uncertainties in the number of B^+B^-, signal yields and efficiencies. The total fractional uncertainty of the combined measurement is $^{+20.5}_{-24.0}$%, and we measure the branching fraction to be

$$\mathcal{B}(B^- \to \tau^-\bar{\nu}_\tau) = (1.06^{+0.34}_{-0.28}({\rm stat})^{+0.22}_{-0.25}({\rm syst}))\times 10^{-4}.$$

The significance is 4.0σ when all τ decay modes are combined, where the significance is defined as $\Sigma = \sqrt{-2\ln(\mathcal{L}_0/\mathcal{L}_{\rm max})}$, where $\mathcal{L}_{\rm max}$ and $\mathcal{L}_0$ denote the maximum likelihood value and likelihood value obtained assuming zero signal events, respectively. Here the likelihood function from the fit is convolved with a Gaussian systematic error function in order to include the systematic uncertainty in the signal yield.

3. Results from the $\Upsilon(5S)$ Engineering Run

We use a data sample of 1.86 fb^{-1} taken at the $\Upsilon(5S)$ energy of $\sim$ 10869 MeV. The experimental conditions of data taking at $\Upsilon(5S)$ are identical to that for $\Upsilon(4S)$ or continuum running. The data sample of 3.67 fb^{-1} taken in the continuum at an energy of 60 MeV below the $\Upsilon(4S)$ was also used in this analysis for comparison.

	$N_{\rm side}^{\rm obs}$	$N_{\rm side}^{\rm MC}$	$N_{\rm sig}^{\rm MC}$	$N_{\rm obs}$	$N_{\rm s}$	$N_{\rm b}$	$\varepsilon^{\rm sel}(\%)$	$\mathcal{B}(10^{-4})$	Σ
$\mu^-\bar{\nu}_\mu\nu_\tau$	96	94.2 ± 8.0	9.4 ± 2.6	13	$5.4^{+3.2}_{-2.2}$	$9.1^{+0.2}_{-0.1}$	8.88 ± 0.05	$1.01^{+0.59}_{-0.41}$	2.0σ
$e^-\bar{\nu}_e\nu_\tau$	93	89.6 ± 8.0	8.6 ± 2.3	12	$3.9^{+3.5}_{-2.5}$	$9.2^{+0.2}_{-0.2}$	8.18 ± 0.05	$0.79^{+0.71}_{-0.49}$	1.3σ
$\pi^-\nu_\tau$	43	41.3 ± 6.2	4.7 ± 1.7	9	$3.4^{+2.6}_{-1.6}$	$4.0^{+0.2}_{-0.1}$	5.79 ± 0.04	$0.96^{+0.74}_{-0.46}$	1.9σ
$\pi^-\pi^0\nu_\tau$	21	23.3 ± 4.7	5.9 ± 1.9	11	$6.2^{+3.9}_{-2.7}$	$4.2^{+0.3}_{-0.3}$	8.32 ± 0.08	$1.23^{+0.77}_{-0.53}$	2.3σ
$\pi^-\pi^+\pi^-\nu_\tau$	21	18.5 ± 4.1	4.2 ± 1.6	9	$3.1^{+3.1}_{-2.6}$	$3.7^{+0.3}_{-0.2}$	1.75 ± 0.03	$2.99^{+3.01}_{-2.49}$	1.2σ
Combined	274	266.9 ± 14.3	32.8 ± 4.6	54	$21.2^{+6.7}_{-5.7}$	$30.2^{+0.5}_{-0.4}$	32.92 ± 0.12	$1.06^{+0.34}_{-0.28}$	4.0σ

Table I The number of observed events in data in the sideband region ($N_{\rm side}^{\rm obs}$), number of background MC events in the sideband region ($N_{\rm side}^{\rm MC}$) and the signal region ($N_{\rm sig}^{\rm MC}$), number of observed events in data in the signal region ($N_{\rm obs}$), number of signal ($N_{\rm s}$) and background ($N_{\rm b}$) in the signal region determined by the fit, signal selection efficiencies ($\varepsilon^{\rm sel}$), extracted branching fraction ($\mathcal{B}$) for $B^- \to \tau^-\bar{\nu}_\tau$. The listed errors are statistical only. The last column gives the significance of the signal including the systematic uncertainty in the signal yield (Σ).

The B_s mesons are produced at the $\Upsilon(5S)$ through the intermediate $B_s\bar{B}_s$, $B_s^*\bar{B}_s$, $B_s\bar{B}_s^*$ or $B_s^*\bar{B}_s^*$ pair production channels, where B_s^* decays to $B_s\gamma$. These intermediate channels can be distinguished kinematically and their production ratios can be obtained from the reconstruction of exclusive B_s decays. To improve the statistical significance of our exclusive B_s signal, we combined the six modes $B_s \to D_s^+\pi^-$, $B_s \to D_s^{*+}\pi^-$, $B_s \to D_s^+\rho^-$, $B_s \to D_s^{*+}\rho^-$, $B_s \to J/\psi\phi$ and $B_s \to J/\psi\eta$,which have large reconstruction efficiencies and are described by unsuppressed conventional tree diagrams.

Six conventional B_s decays to $D_s^+\pi^-$, $D_s^+\rho^-$, $D_s^{*+}\pi^-$, $D_s^{*+}\rho^-$, $J/\psi\phi$ and $J/\psi\eta$ final states and four rare B_s decays to K^+K^-, $\phi\gamma$, $\gamma\gamma$ and $D_s^{(*)+}D_s^{(*)-}$ final states are reconstructed. The signals can be observed using two variables: the energy difference $\Delta E = E_{B_s}^{\rm CM} - E_{\rm beam}^{\rm CM}$ and beam-constrained mass $M_{\rm bc} = \sqrt{(E_{\rm beam}^{\rm CM})^2 - (p_{B_s}^{\rm CM})^2}$; $E_{B_s}^{\rm CM}$ and $p_{B_s}^{\rm CM}$ are the energy and momentum of the B_s candidate in the CM system and $E_{\rm beam}^{\rm CM}$ is the CM beam energy. The B_s mesons can be produced at the $\Upsilon(5S)$ energy via the intermediate $e^+e^- \to B_s^{(*)}\bar{B}_s^{(*)}$ channels, with $B_s^* \to B_s\gamma$. The B_s signal regions in $M_{\rm bc}$ and ΔE are separated for different intermediate channels.

After all selections, the dominant background is from $e^+e^- \to q\bar{q}$ continuum events ($q = u,\ d,\ s,$ or c). The distribution of data in $M_{\rm bc}$ and ΔE for the $B_s \to D_s^+\pi^-$ decay mode is shown in Figure 3a. Three D_s^+ decay modes, $\phi\pi^+$, $\bar{K}^{*0}K^+$ and $K_S^0K^+$, are used to reconstruct B_s candidates. Nine events are observed within the B_s signal ellipsoidal region corresponding to $B_s^*\bar{B}_s^*$ pair production channel. Only one event is observed in the B_s signal region for $B_s^*\bar{B}_s + B_s\bar{B}_s^*$ channels, and no events are observed for $B_s\bar{B}_s$ channel. Background outside the signal regions is small and corresponds to 0.1 event for any of three signal regions. The inclusive studies at the $\Upsilon(5S)$ found that $92,000 \pm 7,900 \pm 23,500$ $B_s^{(*)}\bar{B}_s^{(*)}$ pairs are contained within that 1.86 fb^{-1} $\Upsilon(5S)$ data sample. Using this value, we measure the branching fraction to be $\mathcal{B}(B_s \to D_s^+\pi^-) = (0.65 \pm 0.21 \pm 0.19)\%$.

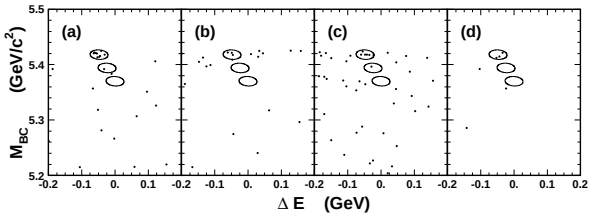

Figure 3: The $M_{\rm bc}$ and ΔE scatter plot for $B_s \to D_s^+\pi^-$(a), $B_s \to D_s^{*+}\pi^-$(b) and $B_s \to D_s^{(*)+}\rho^-$(c) decay modes are shown, where D_s^+ meson is reconstructed in the $D_s^+ \to \phi\pi^+$, $D_s^+ \to \bar{K}^{*0}K^+$ and $D_s^+ \to K_S^0K^+$ decay modes. Also $M_{\rm bc}$ and ΔE scatter plot (d) is shown for the $B_s \to J/\psi\phi$ and $B_s \to J/\psi\eta$.

The $M_{\rm bc}$ and ΔE scatter plots are also obtained for the $B_s \to D_s^{*+}\pi^-$ (Figure 3b) and $B_s \to D_s^{(*)+}\rho^-$ (Figure 3c) decay modes. Again, three D_s^+ decay modes, $\phi\pi^+$, $\bar{K}^{*0}K^+$ and $K_S^0K^+$, are used to reconstruct B_s candidates. The numbers of events within the B_s signal region for the $B_s^*\bar{B}_s^*$ pair production channel are 4 for $B_s \to D_s^{*+}\pi^-$ decay and 7 for $B_s \to D_s^{(*)+}\rho^-$ decay.

The scatter plot in $M_{\rm bc}$ and ΔE for the $B_s \to J/\psi\phi$ and $B_s \to J/\psi\eta$ decays is shown in Figure 3d. One of the observed $B_s \to J/\psi\phi$ candidates is reconstructed in the $J/\psi \to \mu^+\mu^-$ mode and one in the $J/\psi \to e^+e^-$ mode. These two candidates correspond roughly to a branching fraction of $\sim 1 \times 10^{-3}$, in agreement with expectations.

The B_s and B_s^* masses can be extracted from the $M_{\rm bc}$ fits in the $B_s^*\bar{B}_s^*$ channel. The $M_{\rm bc}$ distribution for this channel (Figure 4a) is obtained choosing candidates within the $-0.08 < \Delta E < -0.02$ MeV range. The distribution, shown in Figure 4a, is fitted by the sum of a Gaussian to describe the signal and the ARGUS function to describe the background. The fit

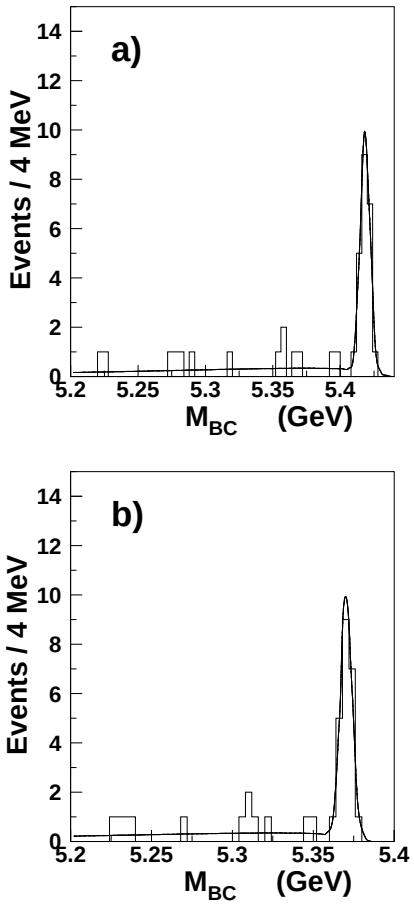

Figure 4: The B_s^* (a) and B_s (b) mass distributions for events within the $-0.08 < \Delta E < -0.02$ MeV interval, corresponding to the $B_s^*\bar{B}_s^*$ channel.

yields the mass value $M(B_s^*) = 5418 \pm 1$ MeV/c^2. The observed width of the B_s signal is 3.6 ± 0.6 MeV/c^2 and agrees with the value obtained from the MC simulation. Using events from the $B_s^*\bar{B}_s^*$ channel we can obtain also the B_s mass (Figure 4b). The distribution shown in Figure 4b is fitted to the sum of a Gaussian and the ARGUS function. The fit yields the B_s mass $M(B_s) = 5370 \pm 1 \pm 3$ MeV/c^2 and width $\sigma(B_s) = 3.6 \pm 0.6$ MeV/c^2.

Additionally, we searched for several B_s rare decays for the first time: the penguin decay $B_s \to K^+K^-$, the electromagnetic penguin decay $B_s \to \phi\gamma$, and the intrinsic penguin decay $B_s \to \gamma\gamma$. We also searched for the tree decay $B_s \to D_s^{(*)+}D_s^{(*)-}$, which is not yet observed and is of special interest because the $D_s^{(*)+}D_s^{(*)-}$ states are expected to be dominantly CP eigenstates. Although the branching fractions for these decays are expected to be too low for observation in this analysis, we obtained upper limits (Table II).

Decay mode	Yield events	Background events	Eff. (%)	upper limit ($\times 10^{-4}$)
$B_s \to K^+K^-$	2	0.14	9.5	3.4
$B_s \to \phi\gamma$	1	0.15	5.9	4.1
$B_s \to \gamma\gamma$	0	0.5	20.0	0.56
$B_s \to D_s^+D_s^-$	0	0.02	0.020	710
$B_s \to D_s^{*+}D_s^-$	1	0.01	0.0090	1270
$B_s \to D_s^{*+}D_s^{*-}$	0	< 0.01	0.0052	2730

Table II The number of events in the signal region, estimated background events and upper limits on the 90% confidence level for $B_s \to K^+K^-$, $B_s \to \phi\gamma$, $B_s \to \gamma\gamma$ and $B_s \to D_s^{(*)+}D_s^{(*)-}$ decay modes.

Acknowledgments

The author wish to thank the KEKB accelerator group for the excellent operation of the KEKB accelerator.

References

[1] S. Eidelman *et al.* (Particle Data Group), Phys. Lett. B **592**, 1 (2004).
[2] W. S. Hou, Phys. Rev. D **48**, 2342 (1993).
[3] B. Aubert (BABAR Collaboration), Phys. Rev. D **73**, 057101 (2006).
[4] A. F. Falk and A. A. Petrov, Phys. Rev. Lett. **85**, 252 (2000).
[5] D. Atwood and A. Soni, Phys. Lett. B **533**, 37 (2002).
[6] D. M. J. Lovelock *et al.*, Phys. Rev. Lett. **54** 377 (1985).
[7] D. Besson *et al.* (CLEO Collaboration), Phys. Rev. Lett. **54**, 381 (1985).
[8] J. Lee- Franzini *et al.*, Phys. Rev. Lett. **65** 2947 (1990).
[9] A. Abashian *et al.* (Belle Collaboration), Nucl. Instrum. Methods Phys. Res., Sect. A **479**, 117 (2002).
[10] R. Brun *et al.*, GEANT3.21, CERN Report DD/EE/84-1 (1984).
[11] See the EvtGen package home page, http://www.slac.stanford.edu/~lange/EvtGen/.